# Waveguide amplifiers and lasers based on $FASnI_3$ perovskite thin films

**Isaac Suárez, [1] Hamid Pashai Adl, [2] Vladimir S. Chirvony, [2] Jesús Sánchez-Díaz, [3] Rafael S. Sánchez, [3] Iván Mora-Seró, [3] and Juan P. Martínez-Pastor [2]**

[1] *Escuela Técnica Superior de Ingeniería, Universidad de Valencia, Valencia 46100, Spain*

[2] *UMDO, Instituto de Ciencia de los Materiales, Universidad de Valencia, Valencia 46980, Spain*

[3] *Institute of Advanced Materials (INAM), Universitat Jaume I, Castelló de la Plana, Castelló 12006, Spain*
**e-mail: isaac.suarez@uv.es, sero@uji.es, juan.mtnez.pastor@uv.es*

**ABSTRACT**

In this work, high-quality polycrystalline formamidinium tin iodide ($FASnI_3$) perovskite thin films are integrated into rigid and flexible substrates to demonstrate optical amplification and lasing. With an appropriate low-temperature treatment and polymethylmethacrylate (PMMA) clapping, the $FASnI_3$ films exhibited remarkable stability and an efficient emission at room temperature. These layers were properly incorporated on rigid ($SiO_2$/Si) and a flexible polyethylene terephthalate (PET) substrate and cladded by a polymethylmethacrylate (PMMA) thin film. The structures conformed to a planar waveguide whose geometrical parameters (i.e. thicknesses of the films) are carefully chosen to demonstrate the generation of amplified spontaneous emission and random lasing modes with extremely low thresholds, 100 nJ/cm$^2$ and 1 µJ/cm$^2$ on rigid and flexible substrates, respectively. In a second device, the $FASnI_3$ films are incorporated as an active medium in a distributed Bragg reflector properly designed to achieve optical resonance at the ASE wavelength. This architecture conforms to an optical cavity able to demonstrate the generation of lasing action with peaks narrower than 1 nm. The proposed devices represent an important step towards the development of future cheap and green photonic technology based on Sn perovskites.

**Keywords**: lead free perovskite, $FASnI_3$, waveguide, random laser, distributed Bragg reflector

## 1. INTRODUCTION

The family of Sn-perovskites has recently emerged as a less toxic set of compounds for future eco-friendly photonic technology [1]. With an extraordinary quantum yield of emission at room temperature, bandgap tunability with the composition, and straightforward incorporation in optical architectures by chemical methods, the $ASnX_3$ (A is an organic/inorganic anion and X is a halide) perovskite represents a suitable nontoxic material to implement lasers, optical amplifiers or light emitting diodes, among other devices. However, since $Sn^{2+}$ is easily oxidized into $Sn^{4+}$ losing its optoelectronic properties, there are few reports providing stable performances with $ASnX_3$ compounds [2-3]. In this way, we successfully developed a low-temperature treatment to fabricate $FASnI_3$ (FA, formamidinium) thin films with good homogeneity and remarkable stability under ambient conditions [4]. The resulting layers exhibited excellent features to implement active devices, such as high absorption above the bandgap, an efficient generation of photoluminescence (PL) at room temperature, or the generation of amplified spontaneous emission (ASE) and traces of random lasing (RL) action under nanosecond pulsed (ns) excitation [5]. At these conditions, this work proposed edge and surface-emitting lasers based on the integration of $FASnI_3$ thin films in rigid and flexible substrates [6]. These layers were firstly deposited on a $SiO_2$ substrate to conform to an optical waveguide whose geometrical parameters (i.e. thicknesses of the films) are properly designed to optimize the excitation and to enhance the generation of the PL. As a result, ASE is demonstrated with an extremely low threshold, about 100 nJ/cm$^2$, and a strong polarization anisotropy preferable to the transverse electric (TE) polarization. Moreover, the waveguide exhibits narrow lasing lines (< 1 nm) caused by the formation of random cavity loops in the polycrystalline grains. Then, the same structure is implemented in a flexible device using polyethylene terephthalate (PET) substrates. Here, despite the formation of films on a flexible platform is always challenging, the flexible waveguide also shows ASE and RL lines with only a one-fold higher threshold (1 µJ/cm$^2$). In a second approach, the $FASnI_3$ thin films are embedded between two mirrors to construct an optical cavity able to demonstrate surface-emitting lasing, again with narrow linewidths (< 1 nm), low stimulated emission thresholds (10 µJ/cm$^2$) and stable performances over hours. We believe that these results will pave the road towards a new generation of active devices based on lead-free perovskites.

## 2. EXPERIMENTAL METHODS

### 2.1 Design and fabrication of the samples

$FASnI_3$ thin films were deposited in the appropriate substrate and covered by a PMMA layer following the procedure explained elsewhere [4-6]. After the deposition, the films showed homogeneity and a grain size of around 1 mm, see SEM image in Fig. 1a. The resulting semiconductor exhibits a remarkable absorption above the bandgap (1-20 $\mu m^{-1}$), blue line in Fig. 1b, and a PL spectrum centered at 890 nm with a full width at half maximum (FWHM) of 57 nm, red line in Fig. 1b. The geometrical parameters of the rigid (Fig. 2a) and flexible (Fig. 2b) waveguides were chosen according to the mode analysis developed for similar structures [7] in order to: (i) allow the single-mode propagation at the photoluminescence (PL) wavelength, (ii) provide optimum excitation of the $FASnI_3$, (iii) enhance the light-matter interaction in the semiconductor and with it the optical gain, (iv) provide preferable direction for the emitted light and a direct outcoupling. In particular, the thicknesses of the $FASnI_3$ and PMMA were fixed at 0.8 µm and 0.2 µm, respectively [6]. In the vertical cavity laser, the PMMA/ $FASnI_3$ bilayer is deposited on the top of commercial distributed Bragg reflector (DBR) and capped with a Au film (see Fig. 2c). Here, the thicknesses of the layers were chosen to achieve a resonant mode at 890 nm (maximum of the PL of the $FASnI_3$).

(a)
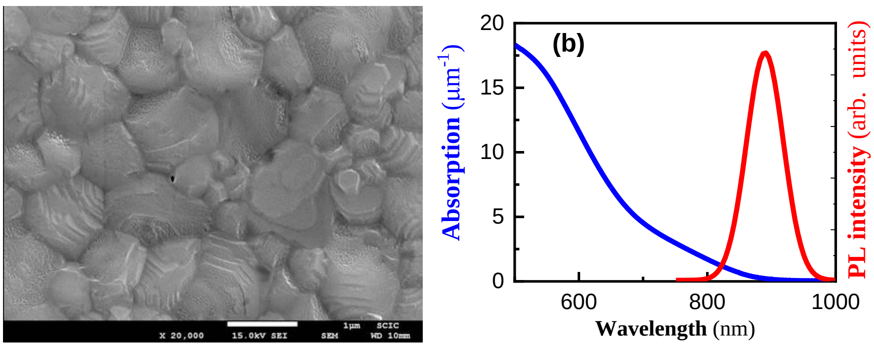


*Figure 1. (a) SEM image of the FASnI3 film. (b) Absorption (solid blue line) and PL (solid red line) spectra measured at room temperature.*

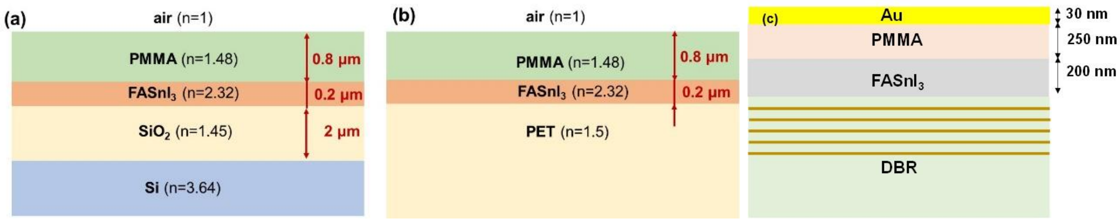


*Figure 2. Architecture of the waveguide geometries used in this work. (a) 200 nm $FASnI_3$ deposited on rigid $SiO_2$ (2 µm)/Si. (b) 200 nm $FASnI_3$ deposited on flexible PET. All samples were covered by a 800 nm PMMA cladding layer. (c) DBR structure incorporating the $FASnI_3$ film.*

### 2.2 Optical characterization

The waveguides and DBR lasers were analyzed by pumping the structures with Nd:Yag laser doubled at 532 nm (1 kHz, 1ns) and collecting the photoluminescence (PL) with a grating spectrograph (DNS-300 from DeltaNu) and detected by a back-illuminated Si CCD (DV420A-OE from Andor) at its exit. All measurements were carried out at room temperature and ambient conditions.

## 3. RESULTS

### 3.1 Edge emitting lasers

Waveguides were characterized by end-fire coupling the excitation beam at the input edge of the sample and collecting the waveguided signal from its output edge [6]. Fig. 3 shows representative spectra obtained in a rigid device (the flexible waveguide presented similar behavior). At low excitation fluences, the waveguided PL shows a Gaussian PL spectrum centered at 890 nm, see Fig. 3a. However, above a threshold of around 0.1-1 $\mu J/cm^2$ the spectrum collapses to a narrow band characteristic of ASE [7]. Interestingly, the ASE band contains narrow lines

(< 1 nm) which are attributed to random lasing action caused by scattering on the polycrystalline grains [6]. Indeed, the log-log plot of the PL as a function of the excitation, Fig. 3b, shows an S-curve characteristic of lasers. Finally, the outcoupled ASE/RL shows a preferable transverse electric (TE) polarization, which enables applications where the control of the polarization is required.

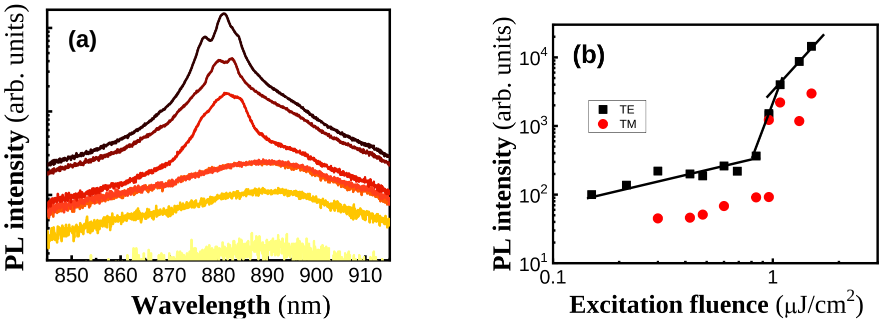


*Figure 3. Demonstration of ASE and RL observed for the waveguiding geometry. (a) PL spectra for different excitation fluences. (b) Log-Log plot of the PL intensity at 890 nm as a function of excitation fluence for TE (black) and TM (red) polarization.*

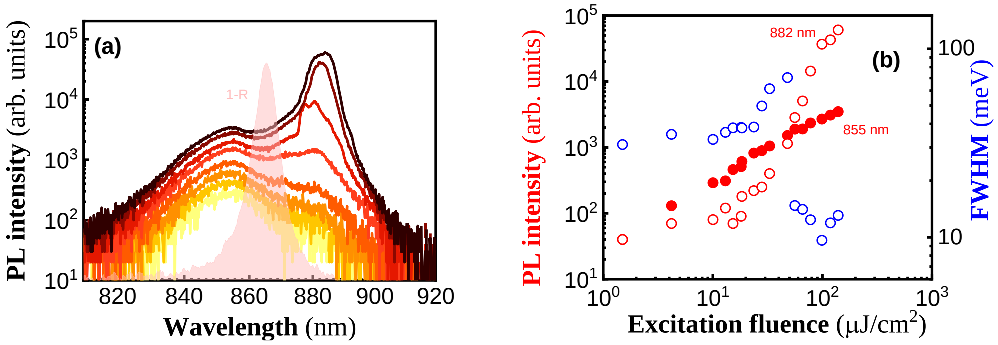


*Figure 4. Vertical cavity laser with a resonant wavelength located at 865 nm (a) PL collected for different excitation fluences. Shadow area correspond to the mode. (b) Evolution of the PL (red symbols) and FWHM (blue symbols) as a function of the excitation fluence.*

### 3.2 Surface emitting lasers

Vertical cavity surface emitting lasers were characterized in transmittance geometry with the experimental conditions described in section 2. Fig. 4a plots the PL spectra in a cavity where the resonant optical mode is located at 866 nm (red dash area). At very low excitation fluences the spontaneous emission spectrum is centered at 855 nm and results from the coupling of the PL to the cavity mode. Above the threshold of stimulated emission, the PL spectrum is dominated by an ASE line at 882 nm exhibiting a superlinear growth (abrupt narrowing down to 10-12 meV), see red (blue in the case of the linewidth) open circles in Fig. 4b. Interestingly, the overlap of the tail of the mode with the stimulated emission region (i.e., with the zone of sufficiently strong positive gain) results in the enhancement of the ASE intensity (see corrugations in Fig. 4a) and the blue-shift of the ASE wavelength compared to that measured in the waveguide geometry (see Fig. 3a). It is also worth mentioning that the stronger interaction of the mode with the excitonic emitted light results on a weaker influence of the RL, because these modes are confined in the transverse direction of the semiconductor while the vertical DBR device emits light through the longitudinal mode. Nevertheless, the log-log plot of the PL intensity as a function of the excitation fluence at the ASE wavelength (882 nm) exhibits the S-curve signature of lasers (open red symbols in Fig. 4b), while the evolution of the PL intensity at 855 nm shows the linear growth characteristic of spontaneous emission (filled red symbols in Fig. 4b). Accordingly, the full width of half maximum (FWHM) of the spectra (blue symbols) in Fig. 4b decreases abruptly above the threshold and reaches a linewidth smaller than 10 meV for the highest excitations.

## 4. CONCLUSIONS

In this manuscript, $FASnI_3$ films were incorporated in edge and surface-emitting devices to demonstrate ASE and RL at room temperature and ambient conditions. First, a waveguide structure was implemented in both rigid and flexible substrates. This configuration imposed a preferable directionality for the RL reducing the ASE threshold and allowing the formation of localized RL loops with high Q factors (Q~1000) and narrow lasing lines (~1 nm). Indeed the stimulated emission threshold is reduced, down to 0.1 and 1.5 $\mu J/cm^2$ in rigid and flexible substrates, respectively. More importantly, the WG shows a preferable TE lasing polarization, which is, to the best of our knowledge, a particular signature for this device not earlier observed for any other RL systems. Then, the $FASnI_3$ films were incorporated inside a vertical mirror-type cavity (bottom DBR and top Au) structure designed to obtain resonant modes close to the ASE band (880-890 nm). The fabricated device presented narrow lasing modes at room temperature above moderate thresholds (10 $\mu J/cm^2$). These results represent a new approach towards a future photonic technology based on lead-free perovskites.


## ACKNOWLEDGEMENTS

This project received funding from the European Union's Horizon 2020 research and innovation programme under grant agreement No 862656 (project DROP-IT) and the European Research Council (ERC) via Consolidator Grant (724424, No-LIMIT), by the Spanish MINECO through projects no. PID2020-120484RB-I00 and PID2019-107314RB-I00 (Stable), and by Generalitat Valenciana COMCUANTICA/009.


## REFERENCES


[1] R. Wang *et al.*: Opportunities and Challenges of Lead-Free Perovskite Optoelectronic Devices, *Trends Chem*., vol. 1, no. 4, pp. 368–379, 2019.

[2] G. Xing *et al.*: Solution-Processed Tin-Based Perovskite for Near-Infrared Lasing, *Adv. Mater.*, vol. 28, no. 37, pp. 8191–8196, 2016.

[3] H. C. Hsu *et al.*: Room-temperature near-infrared random lasing with tin-based perovskites prepared by cvd processing, J. Phys. Chem. C, vol. 125, no. 9, pp. 5180–5184, 2021.

[4] J. Sanchez-Diaz *et al.*: Tin perovskite solar cells with >1,300 h of operational stability in N2 through a synergistic chemical engineering approach, Joule, vol. 6, no. 4, pp. 861–883, 2022.

[5] V. S. Chirvony *et al.*: Unusual Spectrally Reproducible and High Q-Factor Random Lasing in Polycrystalline Tin Perovskite Films, vol. 35, pp. 2208293 Adv. Mater., 2023.

[6] I. Suárez *et al.*: Directional and Polarized Lasing Action on Pb-free FASnI3 Integrated in Flexible Optical Waveguides, Adv. Opt. Mater., vol. 10, no. 15, p. 2200458, 2022.

[7] I. Suárez *et al.*: Mechanisms of Spontaneous and Amplified Spontaneous Emission in CH3NH3PbI3 Perovskite Thin Films Integrated in an Optical Waveguide, Phys. Rev. Appl., vol. 13, no. 1, p. 064071, 2020.